Extended Abstracts of the 2019 International Conference on Solid State Devices and Materials, Nagoya, 2019, pp761-762

Analysis of Inversion Channel Mobility in a GaN-based MOSFET

Daigo Kikuta[1], Tetsuo Narita[1] and Tetsu Kachi[2]

[1] Toyota Central R&D Labs., Inc.
41-1, Yokomichi, Nagakute
Aichi 480-1192, Japan
Phone: +81-561-71-7507 E-mail: kikuta-d@mosk.tytlabs.co.jp
[2] IMaSS, Univ. of Nagoya
Furo-cho, Chikusa-ku
Nagoya 464-8601, Japan
Phone: +81- 52-789-5934

Abstract

In this study, we discuss suppression mechanisms of the inversion channel mobility in a GaN-based MOSFET with Al_2O_3 gate oxide. The measured effective mobility-vertical surface electric field (μ_{eff} – E_{eff}) curve was far from the curve of Si-MOSFET due to highly interface density, so that we could not extract dominant scattering. The corrected μ_{eff} – E_{eff} curve using ideal C_G – V_G curve instead of measured C_G – V_G curve showed similarities to μ_{eff} – E_{eff} curve of Si-MOSFET. The corrected μ_{eff} was proportional to $E_{eff}^{-2.0}$, which had small temperature dependence in the higher E_{eff} region. These results clearly indicate that the μ_{eff} in the higher E_{eff} region is essentially limited by surface roughness scattering.

1. Introduction

Gallium nitride (GaN) based electron devices have attracted attention as next-generation power devices due to its higher figure of merit than Si or SiC [1]. GaN-based vertical metal-oxide-semiconductor filed-effect transistors (MOSFETs) have been reported from several groups and they showed good transistor characteristics such as high breakdown voltage [2-4].

Channel resistance is one of important parameter to reduce total on-resistance of the MOSFETs. Increasing of permittivity of gate oxide is effective way to reduce the cannel resistance by increasing of channel electron density. Al_2O_3 [5], AlON [6], AlSiO [7] have been proposed as the high-k oxide and they shows good interface property on n-type GaN.

On the other hand, increasing of channel electron mobility is also effective way to reduce the channel resistance. However, there is only a few reports about the inversion channel mobility of GaN-based MOSFET, especially dominant scattering.

In this study, we evaluate inversion channel mobility in a GaN-based MOSFET and clarify the dominant scattering of the channel electron.

2. Device structure and fabrication processes

A schematic cross section of the fabricated MOSFET is shown in Fig. 1. A 3-μm-thick Mg doped p-type GaN was grown on n-type GaN substrate by MOVPE. The concentration of Mg was about 2×10^{17} cm^{-3}. The wafers were annealed at 850 °C in nitrogen to activate Mg. The heavily doped n-type GaN (n^+-GaN) regions were formed by Si ion implantation with activation annealing at 1000 °C for the source and drain regions. A 40-nm-thick Al_2O_3 was deposited by plasma-enhanced atomic-layer-deposition using TMA and O radical as the precursors of Al and O. The Al_2O_3 was annealed at 650 °C in nitrogen as post-deposition annealing. A nickel/gold stack was deposited on the p-type GaN as a p-contact. A 200-nm-thick aluminum film was deposited as a gate electrode. A 260-nm-thick titanium/aluminum/nickel stack was deposited as source and drain electrodes.

The gate length (L_G) and width (W_G) of evaluated MOSFET were 100 μm and 100 μm, respectively.

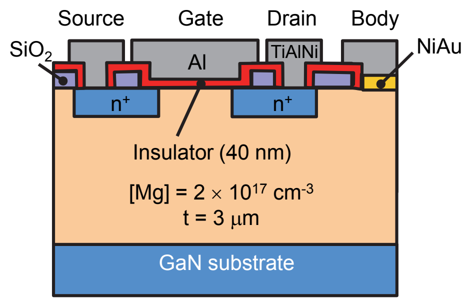

Fig. 1 Schematic cross section of the fabricated MOSFET.

3. Evaluation of inversion channel mobility

To analyze inversion channel mobility, we evaluate effective mobility - vertical surface electric field (μ_{eff} – E_{eff}) characteristic. The μ_{eff} of the channel in fabricated MOSFET was calculated using following equation:

$$\mu_{\mathrm{eff}} = \frac{g_{\mathrm{d}} L_{\mathrm{G}}}{W_{\mathrm{G}} Q_{\mathrm{n}}} \quad (1)$$

where g_d is drain conductance, and Q_n is channel electron density at MOS interface. The E_{eff} in GaN was given by

$$E_{\mathrm{eff}} = \frac{1}{\varepsilon_{\mathrm{GaN}}} \left(\frac{1}{2} Q_{\mathrm{n}} + Q_{\mathrm{dep}} \right) \quad (2)$$

where ε_{GaN} is dielectric constant of GaN, Q_{dep} is charge density in depletion region. Q_n was given by

$$Q_{\mathrm{n}} = \int_{V_{\mathrm{TH}}}^{V_{\mathrm{G}}} C_{\mathrm{G}} dV_{\mathrm{G}} \qquad (3)$$

where C_G is gate capacitance, V_G is gate voltage, and V_{TH} is threshold voltage of MOSFET.

Figure 2 (a) shows the measured $\mu_{eff} - E_{eff}$ curve of the MOSFET (blue curve). The μ_{eff} slowly increased with increasing of E_{eff}. Then the μ_{eff} saturated at about 1.5 MV/cm. In the case of Si-MOSFETs, μ_{eff} increases rapidly with the increase of E_{eff}, after that it decreases with E_{eff} by phonon scattering or surface roughness scattering [8]. The obtained $\mu_{eff} - E_{eff}$ curve differs widely from the curve of Si-MOSFET.

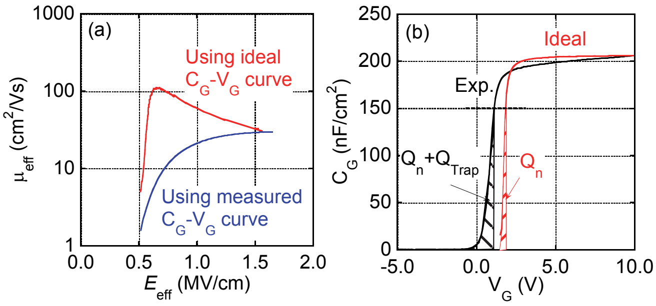

Fig. 2. (a)$\mu_{eff} - E_{eff}$ curves of the MOSFET, (b) Experimental and ideal $C_G - V_G$ characteristics of the MOSFET. In Fig. (a), the blue curve is calculated using measured $C_G - V_G$ curve. The red curve is calculated using ideal $C_G - V_G$ curve.

A similar $\mu_{eff} - E_{eff}$ curve was reported by Zhu *et al* [9]. They revealed an error in mobility extraction due to high density interface trap. A measured $C_G - V_G$ curve contains information of both Q_n and trapped electron density (Q_{Trap}) by interface traps as shown in Fig. 2 (b). Therefore, they proposed correction method using an ideal $C_G - V_G$ curve of the MOSFET instead of the measured $C_G - V_G$ curve to determine the actual channel electron density.

Corrected $\mu_{eff} - E_{eff}$ curve is also shown as a red curve in Fig. 2 (a). An ideal $C_G - V_G$ curve was calculated by Silvaco ATLAS as shown in Fig. 2 (b). The corrected $\mu_{eff} - E_{eff}$ curve increased rapidly with increasing E_{eff}, and then μ_{eff} decreased with increasing E_{eff}. This curve was quite similar to that of the Si-MOSFET.

Figure 3 shows the corrected $\mu_{eff} - E_{eff}$ curves at various measurement temperatures. The μ_{eff} decreased with increasing measurement temperature. In the higher E_{eff} region, the μ_{eff} had a small temperature dependence. And corrected μ_{eff} was proportional to $E_{eff}{}^{-2.0}$.

In the case of Si-MOSFET, the μ_{eff} reduced by surface roughness scattering has no temperature dependence and it is proportional to $E_{eff}{}^{-2}$[8]. These results indicate that the μ_{eff} of the fabricated GaN-based MOSFET was essentially limited by the surface roughness scattering in the higher E_{eff} region.

In the present analysis, the apparent decrease of μ_{eff} involves both such scattering effect and decrease of channel electron density due to capture by interface traps. Therefore, further quantitative investigation of mobility components requires the separation of these effects or essentially suppression of interface traps. In terms of reducing channel resistance, both the surface roughness scattering and the interface trap density should be suppressed.

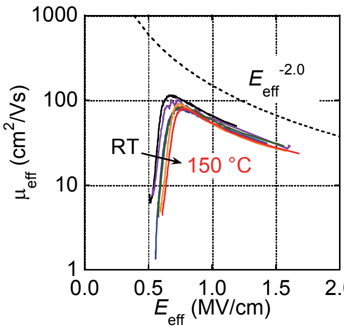

Fig. 3 $\mu_{eff} - E_{eff}$ curves of the MOSFET at different measurement temperature. Measurement temperature was varied from room temperature to 150 °C.

3. Conclusions

In this study, we analyzed inversion channel mobility of GaN-based MOSFET. The measured $\mu_{eff} - E_{eff}$ curve was far from that of Si-MOSFET due to the highly interface trap density. The corrected $\mu_{eff} - E_{eff}$ curve calculated using the ideal $C_G - V_G$ curve showed similarities to the $\mu_{eff} - E_{eff}$ curve of the Si-MOSFET. The corrected μ_{eff} was proportional to $E_{eff}{}^{-2.0}$ and it had small temperature dependence at higher E_{eff} region. These results clearly indicate that the μ_{eff} of the fabricated MOSFET was essentially limited by surface roughness scattering.

Acknowledgements

This work was supported by MEXT "Program for research and development of next-generation semiconductor to realize energy-saving society."

References

[1] T. P. Chow and R. Tyagi, IEEE Trans. Electron Devices **41** (1994) 1481.
[2] M. Kodama *et al.*, Appl. Phys. Express **1** (2008) 021104.
[3] T. Oka et al., Appl. Phys. Express **8** (2015) 054101.
[4] R. Tanaka *et al.*, Appl. Phys. Express **12** (2019) 054001.
[5] T. Hashizume *et al.*, Appl. Phys. Express **11** (2018) 124102.
[6] K. Watanabe *et al.*, Appl. Phys. Lett. **111** (2017) 042102
[7] D. Kikuta *et al.*, J. Vac. Sci. Techol. A **35** (2017) 01B122.
[8] S. Takagi *et al.*, IEEE Trans. Electron Devices **41** (1994) 2357.
[9] W. Zhu, J.-P. Han, and T. P. Ma, IEEE Trans. Electron Devices **51** (2004) 98.